Focal adhesion kinase and paxillin : mediators of breast cancer cell migration

Verkoeijen, S.

CHAPTER 4

Role of Fos-related antigen-1 in focal adhesion kinase-mediated chemoresistance of mammary adenocarcinoma cells

Saertje Verkoeijen [1*], Maroesja J. van Nimwegen [1*], Yafeng Ma [1*], Hans van Dam [2], John H. Meerman [1] and Bob van de Water [1]

[1]Division of Toxicology, Leiden/Amsterdam Center for Drug Research (LACDR), Leiden University, Leiden, the Netherlands
[2]Department of Molecular Cell Biology, Leiden University Medical Center (LUMC), Leiden, the Netherlands
[*]These authors contributed equally to the manuscript.

Running title:
Focal adhesion kinase and breast cancer drug resistance

ABSTRACT

Focal adhesion kinase (FAK) is essential for tumor cell survival, migration and metastasis formation. The exact role and mechanism of FAK in chemoresistance of solid and metastatic tumors remain unclear. Conditional expression of focal adhesion kinase-related non-kinase (FRNK) in established MTLn3 mammary fat pad tumors prior to doxorubicin treatment reduced tumor progression by more than eighty percent. Moreover, in experimental metastasis model doxorubicin treatment combined with FRNK significantly reduced lung metastasis outgrowth by almost seventy percent without affecting metastasis size. Neither FRNK nor doxorubicin alone affected fat pad tumor or lung metastasis growth compared to control conditions. Genome-wide gene expression profiling identified Fra-1, an activator protein (AP)-1 family member, as an essential mediator in this process. Loss of FAK suppressed Fra-1 expression, while loss of Fra-1 reduced cell adhesion and increased stable focal adhesion formation. While Fra-1 knockdown sensitized MTLn3 cells towards doxorubicin, Fra-1 overexpression suppressed cell death when FAK was absent. A model is proposed wherein FAK-mediated signaling is linked to Fra-1 expression and cell survival thereby modulating drug resistance.

INTRODUCTION

Chemoresistance of distant tumor metastases is a major problem in the treatment of cancer. This is mainly due to increased and unsuppressed proliferation and survival signaling of cancer cells. Increased expression of the non-receptor tyrosine kinase focal adhesion kinase (FAK) is implicated in various tumors, including breast tumors (1,2). FAK expression is positively associated with breast cancer development and poor disease prognosis (3,4). The accumulative data indicate an essential role for FAK in tumor cell migration, invasion, proliferation and survival processes enhancing the metastatic capacity of tumor cells and possibly also a resistant phenotype (5-7).

Once cells adhere to the extracellular matrix (ECM), tyrosine phosphorylation of multiple FAK residues and consequent protein-protein interactions result in the activation of survival signaling pathways (8,9). Inhibition of FAK by siRNA or expression of FAK deletion mutants, including FRNK or FAT, results in the onset of apoptosis itself and/or sensitization to anticancer drug treatment in a variety of cancer cell types *in vitro* including breast cancer cells (10-12). Furthermore, systemic RNA interference-based FAK knockdown inhibits ovarian tumor growth and increases sensitivity towards docetaxel and cisplatin (13-16). However, given the non-directed targeting of the siRNAs, it remains unclear whether these effects are related to direct effects on tumor, stromal or vascular endothelial cells. So far a direct relationship between specific inhibition of FAK function in tumor cells *in vivo* and sensitization towards anticancer drugs needs to be established. Moreover, it remains unclear whether such a role for FAK would be similar in primary tumors and in distant metastases.

Fra-1 (Fos-related antigen 1, also named Fosl-1), is a component of activator protein (AP)-1 transcription factor. The AP-1 transcription factor complex consists of Fos, Jun and ATF family members (17). It plays a critical role in regulating tumor cell proliferation, survival, migration and invasion through modulation of genes expression of for example cyclin dependent kinases, cyclins, metalloproteinases and adhesion molecules. Fra-1 expression is associated with breast cancer (18-20) with low expression in ER-positive luminal-like breast cancer cells and high expression in migratory mesenchymal-like breast cancer cells (19,20). Overexpression of Fra-1 in epithelial-like breast cancer cells promotes cell proliferation (19). Fra-1 is essential for the migratory and invasive behavior of

different cancer cells (19,21), which in colon carcinoma cells is related to the suppression of beta1-integrin activation, thereby preventing initiation of RhoA/ROCK-dependent contractility and focal adhesion stabilization (21). In addition, Fra-1 expression is linked to the control of cell survival in different cell types (22,23). So far the relationship between FAK and Fra-1 signaling in susceptibility towards anticancer drugs remains unclear.

To investigate sensitization towards anticancer drugs as a consequence of selective tumor cell-related FAK inhibition in the *in vivo* situation, conditional inhibition of FAK in tumor cells is required. The rat mammary adenocarcinoma MTLn3 cell line is a good model to study the role of FAK in drug sensitivity, since MTLn3 cells in culture are sensitive towards a variety of anticancer reagents including cisplatin, etoposide and doxorubicin (24,25) but these cells are resistant under *in vivo* conditions ((26) and the present work). Importantly, we have recently established a MTLn3 model to conditionally express FRNK *in vivo* in a doxycyline-dependent manner: MTLn3-tetFRNK cells (7). This allowed us to conditionally modulate FAK function at any given moment without affecting the initial tumor formation and metastasis formation.

Our data indicate for the first time that conditional expression of FRNK in metastatic MTLn3 breast tumor cells sensitizes both primary tumors in the mammary fat pad as well as experimental lung metastases towards doxorubicin treatment. Gene expression profiling of MTLn3-tetFRNK cells identified Fra-1 as a target for FAK-mediated signaling. While RNAi-mediated FAK knockdown also suppressed Fra-1 expression, knockdown of Fra-1 did not affect FAK expression but did sensitize MTLn3 cells towards doxorubicin-induced apoptosis. Moreover, overexpression of Fra-1 inhibited the sensitization to doxorubicin when FAK was suppressed. Our data support a model whereby FAK signaling drives Fra-1 expression, thereby modulating the sensitivity towards anticancer drugs.

MATERIALS AND METHODS

Chemicals and antibodies

Alpha modified minimal essential medium without ribonucleosides and deoxyribonucleosides (α-MEM), fetal bovine serum (FBS), phosphate-buffered saline (PBS), trypsin, Lipofectamine-Plus and geneticin (G418 sulphate) were from Life Technologies. Doxorubicin and doxycycline were from Sigma. Hoechst 33258

and the Alexa-488 protein labeling kit were from Molecular Probes. Hygromycin was from Roche. All other chemicals were of analytical grade. Primary antibodies were anti-HA (clone 3F10) and anti-HA (clone 12CA5) (Roche), anti-FAK (Upstate, Lake Placid, NY), anti-Fra-1 (Santa Cruz Biotechnology), anti-myc (Roche), anti-phospho-ERK (Cell Signalling), anti-active caspase-3 (New England Biolabs), anti-paxillin (Transduction), anti-paxillin-PY118 and anti-FAK-PY397 (Biosource).

Cell culture, stable cell lines and transient knockdown

MTLn3 rat mammary adenocarcinoma cells and MTLn3-tetFRNK cells were cultured as previously described (7). To establish retrovirally-transduced stable cell lines, the construct pBABE-puro-Fra-1 tagged with 8xmyc (27) was used. pBABE-puro empty vector was used as a control. MTLn3 cells were infected by retrovirus in the presence of polybrene (10 μg/ml) overnight. Stable transfectants were obtained by selection in 2 μg/ml puromycin for 1 week. Cells were transfected with smartpool siRNA mixes (Dharmacon) against FAK or Fra-1 (50 nM) using Dharmafect reagent 2. siRNA against GFP was used as control. All experiments were performed 48-72 hr post-transfection.

***In vitro* doxorubicin exposure and cytotoxicity assays**

For cell death analysis, after 24 hours of pre-incubation with doxycycline to express HA-FRNK, cells were exposed to 2 μM doxorubicin (or DMSO as a control) in α-MEM for 8 hours. Cell death was determined by staining the pooled attached and detached cells for Annexin-V-Alexa488/Propidium Iodide (AV/PI) as previously described (24). For apoptosis analysis, cells were exposed to 2 μM doxorubicin (or DMSO as a control) for 1 hour in Hanks' balanced salt solution/HEPES, followed by recovery of the cells in α-MEM containing 2.5% (v/v) FBS for an additional 7 hours. Apoptosis was determined with cell cycle analysis as previously described (28) on a FACS-Calibur (BD Biosciences) and expressed as the percentage of cells in sub-G0. For soft agar colony growth assays, MTLn3-tetFRNK cells were cultured for 24 hr in the absence or presence of doxycycline and exposed for 1 hour in Hank's/HEPES buffer to different concentrations of doxorubicin (0, 0.01, 0.05, 0.1, 0.5, 1 and 5 μM). The cells were allowed to recover in α-MEM (2.5% (v/v) FBS). After 24 hours, 12,500 viable cells (resuspended in 1 ml α-MEM containing 0.33% (w/v) agar, 5% (v/v) FBS and PSA) were plated on

top of a bottom agar layer (2.5 ml of α-MEM containing 0.66 % agar, 5% (v/v) FBS and PSA). After two weeks, cells were stained with MTT and the number of colonies was quantified using Image J as previously described (29).

***In vivo* tumor growth, metastasis formation and doxorubicin treatment**

Primary tumors and experimental metastases were induced as described previously (5). Briefly, 1x105 viable cells in 0.2 ml PBS were injected into the lateral tail vein or 1x106 cells in 0.5 ml PBS were injected into the fat pad of female Fischer 344 rats. Nine days after injection of the cells, doxycycline (400 mg/ml in 2.5% (w/v) sucrose) was added to the drinking water; control animals received 1.5% (w/v) sucrose in their drinking water which resulted in equal drinking volumes. Three days later animals were treated either with 6 mg/kg doxorubicin or with PBS (i.p.). After 33 (primary tumor) or 28 days (experimental lung metastases) animals were anesthetized with pentobarbital and the primary tumor or the lungs were excised and the weight was determined, tumors and lungs were fixated (5). After ink injection of the lungs, the number of lung surface metastases was counted. Lung metastasis size was determined by classification of the size of the metastases in H&E-stained lung sections into five groups: ranging from 1 (small) to 5 (large).

Gene expression profiling

Cells were pretreated with doxycycline for 24 hours to induce FRNK expression. Total RNA was isolated with the Qiagen RNAeasy mini-kit and digested with RNase-free DNase (Sigma). Eluted RNA was checked by lab-on-a-chip analysis. mRNA was converted to cDNA and subsequently to digoxigenin-labeled cRNA with a NanoAmpTM RT-IVT labeling kit (Applied Biosystems). Digoxigenin-labeled cRNA samples were hybridized to the microarrays (Applied Biosystems Rat Genome Survey Microarrays) and detected with a Chemiluminescent detection Kit (Applied Biosystems). After conversion of the raw signals of the microarrays to expression values by Expression Array System Analyzer Software Version 1.1.1, a filtering step was applied based on a signal-to-noise ration of >3. Out of all 26,848 genes on the array, 13,206 (49.1%) passed this step and were regarded as expressed in the MTLn3 cells. The probe-to-gene annotation release version 12_05 was used for gene annotation. Subsequently, a median-normalization step was performed by computing a gene-by-gene difference between individual array and the reference array (the array whose overall log-intensity is the median of all array overall log-

intensities), and subtracting the median difference from the log-intensities on that array, so that the gene-by-gene difference between the normalized array and the reference array is 0. BRB-array software tools (http://linus.nci.nih.gov/BRB-ArrayTools.html) were used to identify genes that were differentially expressed among classes by using a multivariate permutation test and random variance F-statistics. Global-test gene ontology (GO) analysis with GoMinertool (http://discover.nci.nih.gov/gominer/) was performed to analysis groups of genes whose expression was differentially regulated among different treatments.

Quantitative RT-PCR

cDNA was synthesized from RNA using oligo(dT)12-18 primers and Superscript reverse transcriptase (Invitrogen Life Technologies). The sequence-specific primer pairs were separately designed by online primer design tools (https://www.genscript.com/ssl-bin/app/primer and http://frodo.wi.mit.edu/cgi-bin/primer3/primer3_www.cgi) and ordered from Biolegio (Nijmegen). The following primer sets were used:

Fra-1 (NM_012953): left: 5'-AGAGCTGCAGAAGCAGAAGG-3', right: 5'-CAAGTACGGGTCCTGGAGAA-3', length: 182 bp. JunB (NM_021836): left: 5'-ATCACGACGACTCATACGCA-3', right: 5'-CGATAAGGATCTGCCAGGTT-3' length: 248 bp. Internal standard, β-actin (NM-031144): left: 5'-CAGCTTCTCTTTAATGTCACGCA-3', right: 5'-TGACCGAGCGTGGCTACA-3', length: 71 bp.

Quantitative RT-PCR was performed on ABI7700 system with the SYBR Green PCR Master Mix kit (Applied Biosystems).

Fluorescence recovery after photobleaching (FRAP) and random migration

To determine cytoplasmic mobility of GFP-paxillin, a 1.8 μm-wide strip spanning approximately the width of the cytoplasm (without any focal adhesions) was photobleached by a short bleach pulse (100 ms) at 100% laser intensity (120 to 160 μW; argon laser at 488 nm). Recovery of fluorescence within the strip was monitored using 100 ms intervals and low laser intensity (450 to 750 nW) to avoid photobleaching by the probe beam. Approximately 10 cells were averaged to generate one FRAP curve for a single experiment. To determine the turnover of individual focal adhesions, photobleaching was applied to a small area covering a single focal adhesion for 1 s with laser intensity of 50 μW. Redistribution of

fluorescence was monitored with 100 ms intervals at 7.5 μW starting directly after the bleach pulse. Approximately 20 focal adhesions (each in distinct cells) were averaged to generate one FRAP curve for a single experiment. All measurements were performed at 37 °C using a heating stage with feedback temperature control and the experiments were performed on at least three different days. Images were analyzed with Image Software (Zeiss). The relative fluorescence intensity of individual focal adhesions was calculated at each time interval as follows: Irel(t) = (FAt / FA0), where FAt is the intensity of the focal adhesion at time point t after bleaching and FA0 is the average intensity of the focal adhesion before bleaching. The fluorescent curves were analyzed with non-linear regression analysis (GraphPad Prism 5) (34).

For live random cell migration, GFP-MTLn3 cells were knocked down with siRNA for 24 hours and seeded on collagen-coated glass bottom plates. Live cell images were captured on the second day in a climate control chamber. Random cell migration was recorded on a Nikon TIRF microscope system (Eclipse TE2000-E, Nikon with automated stage) with framing every 5 minutes for 4 hours using NIS-elements AR software (Nikon).

Immunoblotting and immunofluorescence

Doxorubicin-exposed cells or frozen lung/ tumor tissue were prepared and separated by 7.5% SDS-PAGE and transferred to PVDF membranes (Millipore) as described before (5). Blots were blocked and probed with primary antibody (overnight, 4°C) followed by incubation with secondary HRP-coupled antibody and visualized with ECLplus reagent (Amersham Biosciences, Uppsala, Sweden) on a Typhoon imager 9400 (Amersham Biosciences). Immunostaining of tissue sections and cells was performed as described before (5) and visualization was done on a Bio-Rad Radiance 2100 MP confocal laser scanning system equipped with a Nikon Eclipse TE2000-U inverted fluorescence microscope and a 60X Nikon objective.

Statistical analysis

Student's t test was used to determine significant differences between two means ($p<0.05$).

RESULTS

HA-FRNK expression sensitizes MTLn3 breast tumors to doxorubicin.

To test whether inhibition of FAK sensitizes MTLn3 cells towards doxorubicin treatment under *in vivo* conditions, two Fischer 344 rat models were used: a primary tumor model, in which the tumor cells were injected into the mammary fat pad and an experimental metastasis model, in which the cells were injected into the lateral tail vein. To modulate FAK function we used previously characterized MTLn3-tetFRNK cells that conditionally express the HA-tagged dominant-negative-acting splice variant of FAK, focal adhesion kinase-related non-kinase (FRNK). In both experimental set-ups, HA-FRNK was induced *in vivo* in the tumor cells nine days after injection by addition of doxycycline to the drinking water until the end of the experiment (Fig. 1A and B). Three days after the start of doxycycline treatment, animals were treated either with saline or a sub-lethal dose of doxorubicin (6 mg/kg) (see for experimental setup Fig. 1A). While all animals survived the doxorubicin treatment, doxorubicin caused a temporal and small loss of weight (data not shown) indicative of medium sub-lethal toxicity. Expression of HA-FRNK starting at day nine till the end of the experiment did not affect the growth rate of the primary tumor (Fig. 1C). Also, treatment with 6 mg/kg doxorubicin at day twelve alone was not effective in reducing tumor growth. In contrast, exposure to doxorubicin together with the expression of HA-FRNK caused a significant decrease in tumor growth. This was reflected in the tumor volumes: neither HA-FRNK nor exposure to doxorubicin alone altered the total tumor weight; in contrast, the combination of HA-FRNK and doxorubicin strikingly inhibited tumor growth (Fig. 1D). This indicates that FAK-dependent signaling mediates a resistant phenotype against doxorubicin treatment.

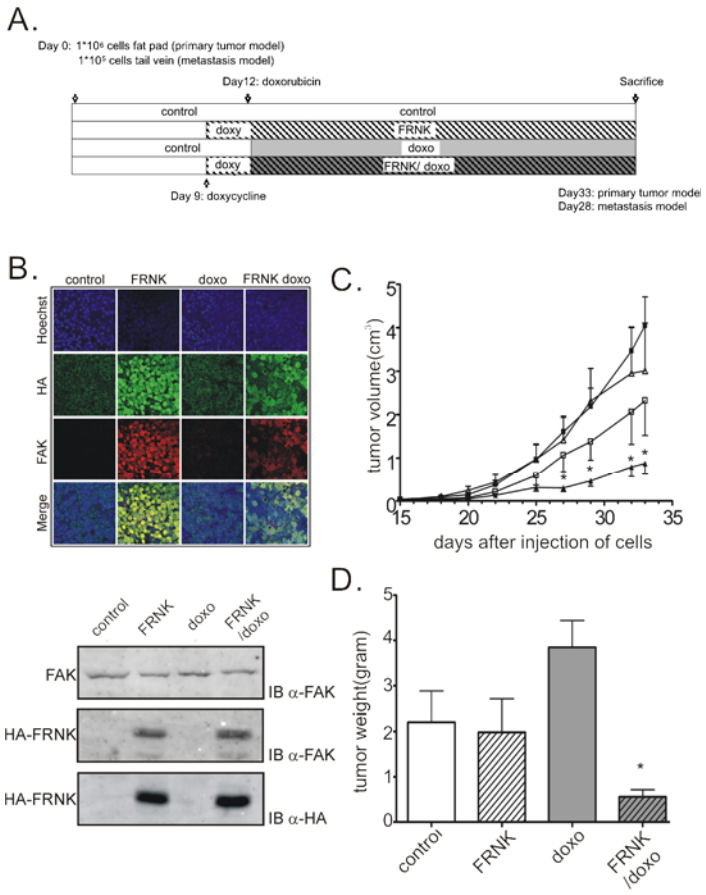

Figure 1. HA-FRNK alleviates doxorubicin resistance of primary MTLn3 tumors. (A) *In vivo* experimental setup for primary tumor and experimental metastasis models as described in detail in Materials and Methods. (B) Primary tumors were isolated, fixed and sectioned and expression of HA-FRNK was determined by fluorescence microscopy and immunoblotting with antibodies against C-terminal FAK and HA. Hoechst staining showed nuclei. (C) During the primary tumor experiment, tumor growth was followed by measuring tumor size as described in Materials and Methods. Open squares: control; filled squares: doxo; open rectangles: FRNK; filled rectangles: FRNK doxo. (D) The weight of the primary tumors was determined.

HA-FRNK sensitizes experimental lung metastases towards doxorubicin treatment.

Chemotherapy is the first line treatment for metastatic breast cancer. The difference in tissue microenvironment between lung metastases and primary tumors may result in differences in survival signaling programs and drug resistance. Therefore, we also investigated whether FAK is involved in resistance of MTLn3 lung metastases. For this purpose MTLn3-tetFRNK cells were injected into the tail vein and after nine days, when micro-metastases were formed, animals were treated with doxycycline. On day twelve animals were treated with doxorubicin (6 mg/kg). The total number of lung metastases was evaluated at the end of the experiment. Doxycycline treatment resulted in conditional expression of HA-FRNK in the majority of lung metastases (Fig. 2A). Neither inhibition of FAK nor exposure to doxorubicin alone reduced the number of lung metastases. In contrast, expression of HA-FRNK followed by doxorubicin treatment three days later did result in a dramatic reduction of the lung tumor burden (Fig. 2B and C). The number of surface metastases was in agreement with the overall lung tumor burden as determined by histopathology (Fig. 2B). Despite the fact that HA-FRNK expression caused a decrease in the number of lung metastases of more than 70% (Fig. 2C), the size of the remaining metastases, irrespective of HA-FRNK expression, was minimally reduced. Hardly any remaining micro-metastases were observed in any of the experimental conditions. Importantly, around 90% of these remaining metastases contained HA-FRNK positive cells, accounting on average for about 50-70% of all cells (Fig. 2D). These data show that the combination of HA-FRNK expression and doxorubicin treatment resulted in elimination of large numbers of micro-metastases, while it did not affect further outgrowth of the remaining metastatic lesions.

FAK signaling regulates Fra-1 expression.

Next, we performed a systematic analysis of HA-FRNK-associated signaling that could explain the sensitization of MTLn3 cells towards doxorubicin. Therefore we performed genome-wide expression profiling in MTLn3-tetFRNK cells; MTLn3 tet-on cells were used as control to exclude potential effects of doxycycline. Out of 13,206 genes expressed in the MTLn3 cells, 494 annotated genes ($p<0.05$, FC>1.5 or <0.67) were differentially expressed upon HA-FRNK expression (individual genes are listed in Supplemental Table 1). Since false discovery rate (FDR) for all

genes was larger than 0.05, we also performed gene ontology (GO) pathway analysis to define alternatively affected biological and molecular pathways and gene sets. 23 GO-groups were identified to be differentially expressed (Table 1).

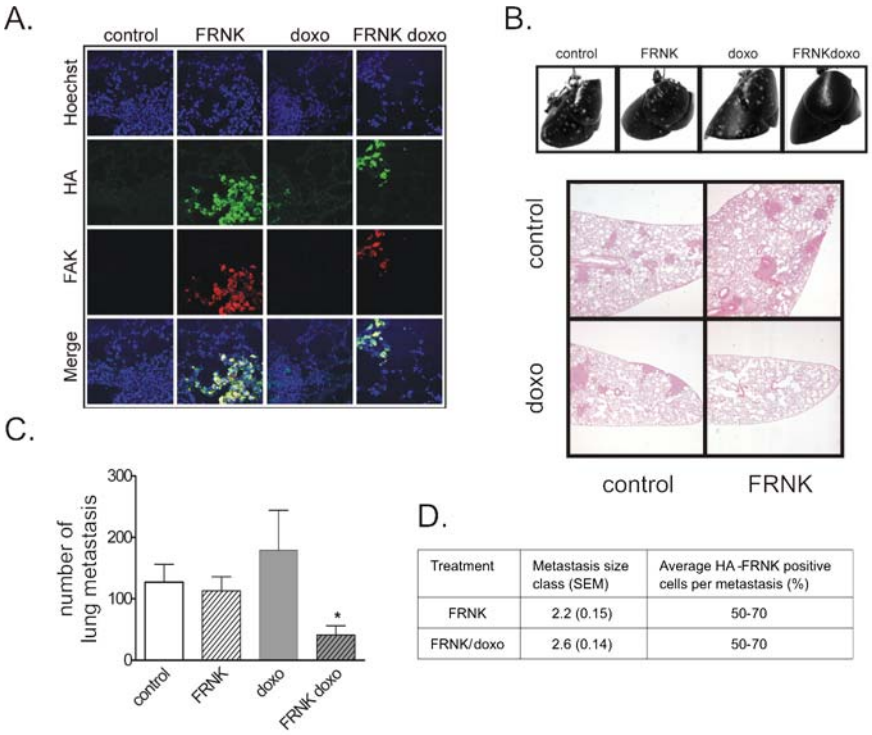

Treatment	Metastasis size class (SEM)	Average HA-FRNK positive cells per metastasis (%)
FRNK	2.2 (0.15)	50-70
FRNK/doxo	2.6 (0.14)	50-70

Figure 2. HA-FRNK sensitizes lung metastases to doxorubicin treatment. Animals were injected with MTLn3-tetFRNK cells and after 9 days rats were exposed to doxycycline or left untreated followed by a single treatment with doxorubicin on day 12. On day 28, animals were sacrificed and lungs were excised. (A) Lungs were evaluated for HA-FRNK expression. (B) Lung metastasis formation was evaluated at macro level on ink-injected lungs (top panel) and at microscopical level on H&E-stained lung tissue sections. (C) The number of surface lung metastases was quantified. (D) The size of the individual remaining metastases and the percentage of HA-FRNK-positive cells in these metastases were determined in lung sections stained for HA-FRNK of animals from the FRNK and FRNK/DOXO groups.

Fra-1 and JunB, both AP-1 family members, were identified as prominently down-regulated genes after HA-FRNK expression and part of the GO-group regulation of transcription (Table 1 and Fig. 3A); other AP-1 family members such as c-Jun and c-Fos were not affected by HA-FRNK expression (Supplemental Fig. 1). Verification of Fra-1 and JunB expression by qRT-PCR showed a 37% decrease of Fra-1 in HA-FRNK-expressing cells compared to controls (Fig. 3B). No significant decrease was observed for JunB. To validate the effect of HA-FRNK, we performed a FAK knockdown with Dharmacon Smartpool siRNA. FAK knockdown in MTLn3 cells significantly reduced Fra-1 mRNA expression by more than 50% as determined by qRT-PCR (Fig. 3C). This was associated with a reduction of Fra-1 protein levels to around 50%. Fra-1 knockdown did not affect the levels of FAK expression (Fig. 3D).

Fra-1 provides cell survival against doxorubicin-induced apoptosis.

Fra-1 has been implicated in cancer progression, cell survival and cell migration. Therefore, we further studied the relationship between FAK and Fra-1 in the context of focal adhesion organization and control of apoptosis. Intriguingly, while Fra-1 knockdown in MTLn3 cells did not affect FAK expression, immunofluorescent-staining of phosphorylated paxillin (Tyr118) followed by quantitative image analysis indicated the presence of larger focal adhesions and increased actin filaments after Fra-1 knockdown (Fig. 4A). This was associated with delayed cell spreading on collagen when the cells were replated (Fig. 4B). Moreover, FRAP experiments with GFP-paxillin-expressing MTLn3 cells demonstrated a stabilization of focal adhesion turnover after Fra-1 knockdown (Fig. 4C). Thus, while the diffusion of GFP-paxillin in the cytoplasm showed no difference after Fra-1 knockdown (control conditions: reduced mobile fraction (Rf) = 0.8851 and half-life (τ) = 0.5498s; Fra-1 knockdown: Rf = 0.8891 and τ = 0.5015s), the turnover of GFP-paxillin at focal adhesions was significantly decreased after Fra-1 knockdown (control conditions: Rf = 0.7560 and τ = 1.239s; Fra-1 knockdown: Rf = 0.7385 and τ = 1.846s). This effect of Fra-1 knockdown on focal adhesion dynamics was associated with reduced cell motility, as determined by analyzing random cell migration of MTLn3 cells (Fig. 4D). Together these data indicate that Fra-1 activity is directly linked to both focal adhesion dynamics, size and cell migration properties, and as such, may also affect signaling mediated at focal adhesions.

Table 1. FRNK-induced alterations in gene ontologies as determined by GO-miner. Analysis: $p<0.05$, upregulation or downregulation in gene ontologies.

Gene Ontology	**p value down**	**genes down**	**p value up**	**genes up**
epidermal cell differentiation			0.01	KA17
B cell differentiation	0.04	CLC, TPD52		
cell cycle	0.03	CDC25B, CDK2, HRASLS3, MAPRE3		
mitosis	0	CDC25B, CDK2, MAPRE3		
regulation of transcription, mitotic	0	***FOSL1, JUNB***		
regulation of cell growth	0.02	WISP1		
negative regulation of cell growth	0.05	NPPB, OKL38		
cell motility			0.05	TPBG
regulation of cell shape	0.05	GNA12, MYH9		
GPI anchor biosynthesis	0.01	GPAA1, PIGM		
protein myristoylation	0.03	NMT2		
protein modification	0	GGCX, PPT2		
protein aminoa acid acylation	0.07	PPARGC1A		
protein sumoylation			0.02	PIAS3
ubiquitin cycle	0.03	RNF40, STAMBP, UBE2D3		
receptor recycling	0.05	RAB40C		
respiraroty chain complex IV			0.02	COX6C
mitochondrial outer membrane	0.04	AKAP1, HK2		
endoplasmic reticulum	0.01	CYP3A13, DDOST, NPL4, NUCB2, TPD53		
endoplasmic reticulum membrane	0	PIGM		
integral to endoplasmic reticulum membrane	0	DHRS9, ELOVL6, SLC35D1		
GPI-anchor transamidase complexes	0.05	GPAA1		
nucleus	0.02	ACTN4, ANKRD1, ANXA7, CDK2, DCK, ETV4***, FOSL1***, HAVCR1, HNRPR, KPTN, MAF, MEF2D, NPL4, NR1H2, NUCB2, PHLDA1, PIM1, PKD1, POU2F2, PPARGC1A, PRKACA, RNF40, STAMBP, TCFE2A, TLE4, TNPO2, WDR3		

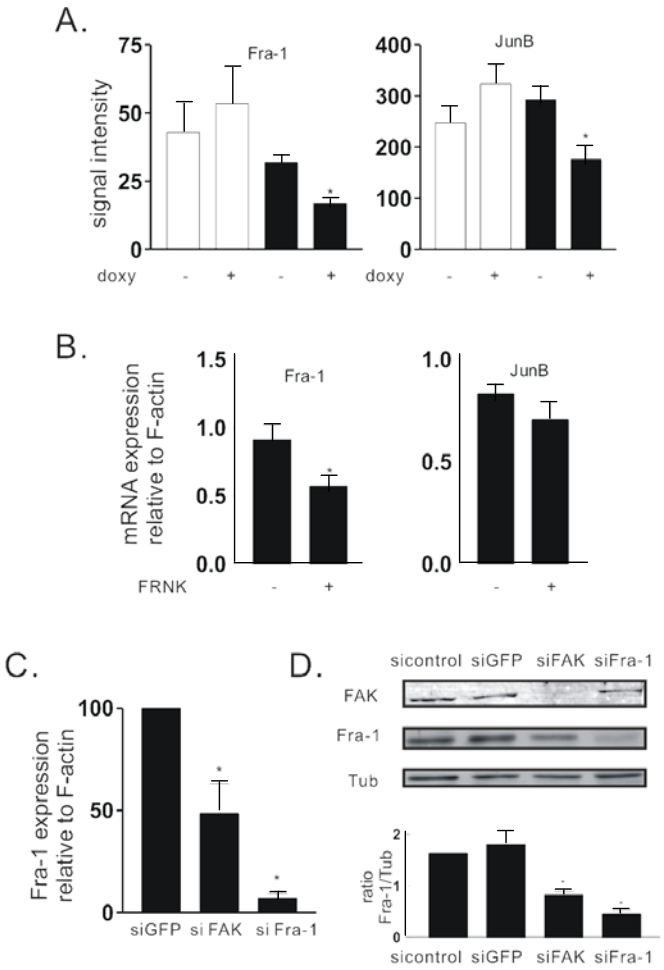

Figure 3. Fra-1 expression is dependent on FAK signaling. Microarray profiling was performed and analyzed as mentioned in Material and Methods. (A) Shown are the expression levels of *fra-1* and *junB* in MTLn3-tet-on (open bars) and MTLn3-tetFRNK cells (closed bars) after O/N treatment with or without doxycycline. (B) *fra-1* and *junB* levels were determined by qRT-PCR in MTLn3-tetFRNK cells with or without O/N treatment with doxycycline (n=3, mean ± SEM; asterisk indicates p=0.017). (C) After treatment of normal MTLn3 cells with siFAK and siFra-1, *fra-1* levels were determined by qRT-PCR (n=3; mean ± SEM; p=0.016). (D) Protein levels of Fra-1 and FAK were determined by immunoblotting; Fra-1 expression levels were quantified by densitometry.

Next we determined the sensitivity of MTLn3 cells towards doxorubicin under conditions where we affected both FAK and Fra-1. Conditional expression of HA-FRNK sensitized MTLn3 cells towards doxorubicin-induced apoptosis (Fig. 5A). Since loss of FAK function decreases Fra-1 expression (Fig 3C and 3D), we hypothesized that Fra-1 loss would also sensitize cells towards apoptosis induced by doxorubicin. Similar to HA-FRNK expression, Fra-1 knockdown sensitized cells towards doxorubicin (Fig. 5B). We anticipated that increased expression of Fra-1 would protect cells against the susceptibility towards doxorubicin-induced apoptosis resulting from the loss of FAK. Therefore we used retroviral vector pBABE-Fra-1 to generate a stable MTLn3 cell line with increased Fra-1 expression (Fig. 5C). Importantly, Fra-1 overexpression did not affect FAK and paxillin levels in MTLn3 cells. Fra-1 overexpression inhibited the onset of apoptosis under conditions where cells were depleted from FAK by siRNA pretreatment (Fig. 5D). All together these data indicate a role for FAK in controlling Fra-1 expression, while Fra-1 expression is essential for cytoprotection against doxorubicin-induced killing of breast tumor cells.

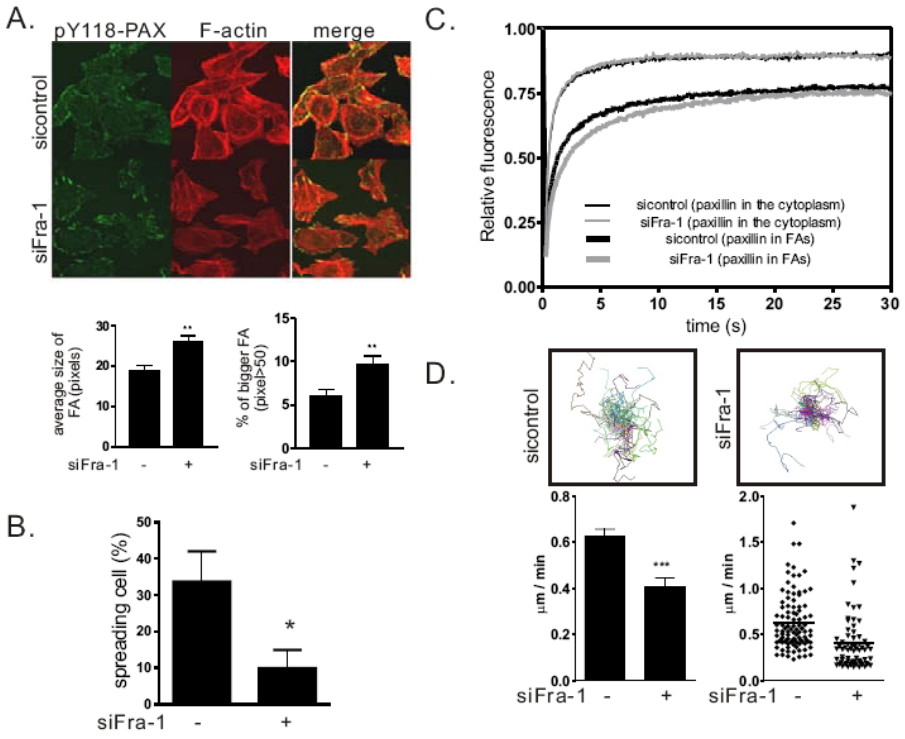

Figure 4. Fra-1 KD affects focal adhesion organization and induces apoptosis of MTLn3 cells. (A) MTLn3 cells were treated with siFra-1 or siGFP for 48 hours and cells were fixed and stained for paxillin-PY118 and F-actin. Following image acquisition by CLSM, the average size of focal adhesions as well as the percentage of large focal adhesions (number of pixels > 50) was determined with ImageProPlus software. (B) siFra-1 knocked down cells were detached and re-seeded on collagen-coated coverslips for 4 hours and cell morphology was observed by phase contrast light microscopy and cell attachment was determined as the percentage of spreading cells. (C) GFP-MTLn3 cells were treated with siFra-1 or sicontrol (siGFP) followed by FRAP analysis on a Zeiss confocal microscope as described in Materials and methods. Shown are representative FRAP curves of GFP-paxillin in the cytosol and at focal adhesions. (D). For random cell migration, knockdown of Fra-1 was performed as described above in GFP-MTLn3 cells. 24 hours after plating, random cell migration was imaged and analyzed as described in Materials and methods. Data shown is mean ± SEM of individual movements, representative of three independent experiments. The top panel indicates the cell tracks of individual cells for sicontrol (left) and siFra-1 (right) conditions.

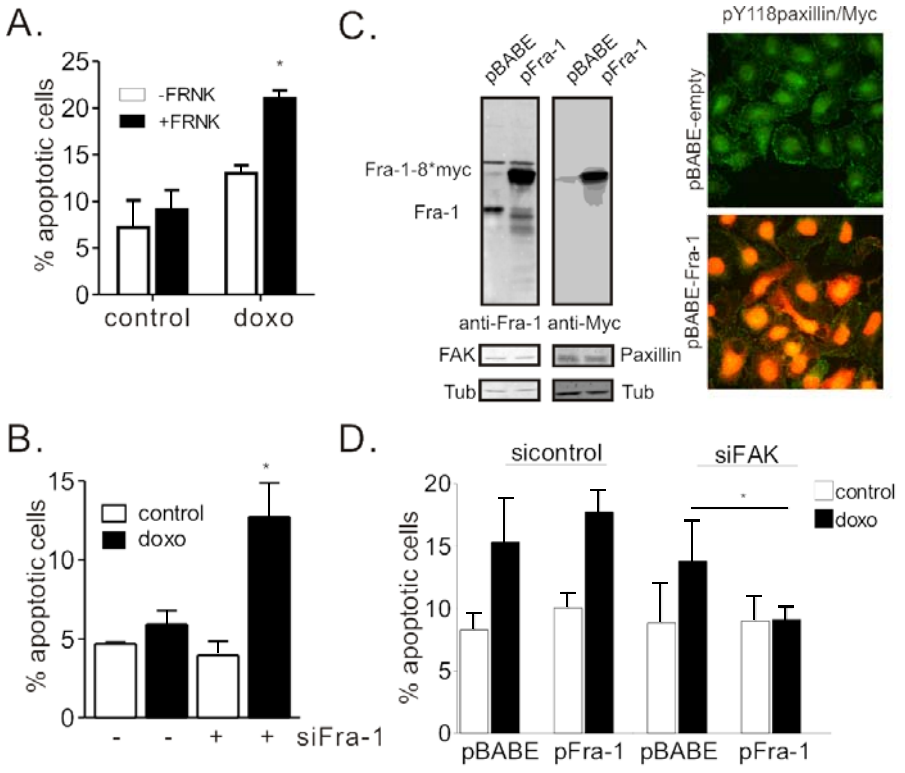

Figure 5. Fra-1 determines sensitivity towards doxorubicin-induced apoptosis. (A) MTLn3-tetFRNK cells were treated overnight with doxycycline to induce HA-FRNK expression and exposed to doxorubicin (2 μM) for 8 hours. Apoptosis was determined with Annexin/PI staining and flow cytometric analysis (n=3; mean ± SEM; asterisk indicates $p<0.05$). (B) MTLn3 cells were treated with siFra-1 or sicontrol for 48 hours followed by treatment with doxorubicin (2 μM) for 8 hours and subsequent apoptosis analysis (n=3; mean ± SEM; asterisk indicates $p<0.05$). (C) MTLn3 cell lines expressing Myc-tagged Fra-1 were generated as described in Materials and methods and characterized for Myc-Fra-1 expression using Western blotting and immunofluorescence. Myc-Fra-1-MTLn3 cells were also analyzed for FAK and paxillin expression. (D) MTLn3-pFra-1 and MTLn3-pBABE control cells were treated with siFAK or sicontrol followed by treatment with doxorubicin (2 μM) for 8 hours and apoptosis was determined as in A and B (n=3; mean ± SEM; asterisk indicates $p<0.05$).

DISCUSSION

Using an orthotopic breast tumor model and an experimental lung metastasis model in combination with conditional doxycycline-dependent expression of a FAK deletion mutant, FRNK, we investigated the role and mechanism of FAK signaling in the regulation of chemo-sensitivity of breast tumor cells towards doxorubicin. We demonstrate that 1) tumor cell-specific inhibition of FAK in both the primary tumor and lung metastases re-sensitizes breast tumor cells towards doxorubicin; 2) induction of FRNK expression selectively affects the expression of a panel of target genes, of which the AP-1 transcription factors Fra-1 and JunB are prominent; and 3) Fra-1 expression in breast tumor cells determines their sensitivity towards doxorubicin. Taken together, these data provide a model wherein FAK-dependent signaling supports the expression of the AP-1 transcription factor Fra-1 thereby providing survival advantages that allow sufficient protection against therapeutically relevant doxorubicin concentrations, resulting in a drug-resistant phenotype. These data support the notion that pharmacological intervention of FAK function will provide opportunities for combined therapy in cancer types that have increased levels of FAK and are resistant against chemotherapy.

Both the orthotopic breast tumor model and experimental metastasis model indicate that HA-FRNK expression ameliorates *in vivo* resistance against doxorubicin. To our knowledge, this is the first time to show that a tumor cell-specific inhibition of FAK enhances drug sensitivity. Although the orthotopic tumor model could not substantiate whether the combined treatment resulted in a complete eradication of subsets of tumor cells or solely in a delay in tumor cell proliferation, our experimental lung metastasis model supports a model wherein the combined treatment kills off micro-metastases completely. While the total number of lung metastases decreased, this was not associated with a clear decrease in the size of the remaining metastases. Importantly, these remaining metastases were in most cases still partly positive for HA-FRNK, indicating that there was not a selection of outgrowth of HA-FRNK-negative cells. By microscopical analysis of HA-FRNK-stained paraffin sections, no remaining micro-metastases were observed, suggesting that FRNK expression rather supported killing of metastatic cells by doxorubicin, than inducing a dormant phenotype of metastasis that were formed up until day twelve after injection of tumor cells. Moreover, our *in vitro* data suggest that conditional HA-FRNK expression facilitates the killing of

MTLn3 cells through apoptosis induced by doxorubcin and thereby prevents long-term colony formation in soft agar assay.

We identified Fra-1 as an important regulator downstream of FAK-mediated survival signaling. Both HA-FRNK expression and FAK knockdown suppressed fra-1 mRNA expression as well as protein levels. In turn, Fra-1 knockdown sensitized MTLn3 cells towards doxorubicin but did not affect FAK expression. Moreover, Fra-1 overexpression inhibited the onset of apoptosis induced by doxorubicin under FAK knockdown conditions, but when FAK was expressed no protection was observed. Fra-1 is a leucine-zipper protein that can dimerize with proteins of the Jun family, thereby forming the transcription factor complex AP-1. Interestingly, JunB was also downregulated after FRNK expression (Fig. 3 and Supplemental Table 2), although this was not significant by qRT-PCR. Based on our microarray data, other Fos and Jun family members have relatively low mRNA expression levels in MTLn3 cells. Therefore, we hypothesize that Fra-1/JunB dimer is an important AP-1 transcription factor complex in these cells. Our previous collaborative work indicates that Fra-1 expression is the most significant differentially expressed gene in a large panel of human breast tumor cells with either an epithelial or a mesenchymal phenotype, and has an over 600-fold higher average expression level in mesenchymal-like breast tumor cells (20). MTLn3 cells also have mesenchymal characteristics and given the fact that mesenchymal-like breast tumor cells typically have a higher metastatic potential (30), we anticipate that such a metastatic and often drug-resistant-associated phenotype may have a FAK-Fra1 signaling axis background.

AP-1 is thought to play an important role in the balance between cell proliferation and apoptosis, the response to genotoxic stress and cell transformation. In colon cancer cells the classical mitogen-activated protein kinase pathway through MEK and ERK is central in the regulation of Fra-1 levels (31). Also, stress conditions such as DNA-damage by UV and cisplatin, induce an ERK-mediated Fra-1 phosphorylation and stabilization by preventing proteasomal degradation (23,31). Possibly, the FAK-mediated regulation of Fra-1 in MTLn3 cells is dependent on modulation of ERK signaling, although we have not been able to identify a differential activity of ERK upon HA-FRNK expression (data not shown). Fra-1 expression seems essential in invasion and motility of tumor cells. This is related to the inactivation of integrin-beta1 by Fra-1 expression in an unknown way (21). This integrin inactivation suppresses activation of the

RhoA/ROCK pathway (21). Also, in MTLn3 cells, ROCK-mediated contractility is enhanced upon Fra-1 knockdown, without affecting the expression of FAK. This is associated with larger and less dynamic focal adhesions. Interestingly, doxorubicin also increases the contractility of MTLn3 cells in a ROCK-dependent manner; however, inhibition of ROCK does not affect doxorubicin-induced apoptosis (data not shown). Since Fra-1 knockdown decreases the dynamics of focal adhesions and therefore most likely also the (survival) signaling at these sites, we anticipate that the stabilization of focal adhesions may be the driving force for sensitization towards doxorubicin. Indeed, FAK-mediated signaling towards the PI3K/PKB pathway seems essential in controlling doxorubicin-induced apoptosis in MTLn3 cells (7). However, at this moment, we can not exclude other possible mechanisms by which Fra-1 acts in concert with focal adhesion signaling to modulate a drug-resistant phenotype. Further research will be essential to unravel the exact mechanism of the Fra-1-mediated control of cell survival in breast cancer cells.

Although we could functionally link modulation of Fra-1 by FAK to drug sensitivity, we can not exclude that other pathways by which FAK signaling modulates drug resistance are also biologically relevant. Indeed, recently, Halder et al. showed that therapy with FAK siRNA in combination with docetaxel reduces tumor growth (13). This effect was attributed to decreased vascularization caused by low VEGF levels. In accordance with this, Mitra et al. showed that inhibition of FAK resulted in reduced VEGF expression and smaller tumors in mice (32). However, our current microarray analysis did not reveal any HA-FRNK-induced downregulation of VEGF/VEGFR pathway components. Moreover, no difference in the vascularization of the primary tumors upon expression of HA-FRNK in either the absence or presence of doxorubicin treatment was observed (unpublished results). Also the small size of the micro-metastases at the time point of doxorubicin exposure in our experimental metastasis model in combination with the already extensive vascularization of lung tissue makes a relationship between VEGF, angiogenesis and drug sensitization unlikely. Our GO-miner-based gene ontology analysis revealed a clear identification of biological programs that are significantly affected by HA-FRNK expression including regulation of mitosis, mitotic regulation of transcription, regulation of cell growth and cell motility (Table 1). Defects in such programs are likely to sensitize cells to doxorubicin. It is still questionable whether the gene expression changes are direct effects of HA-FRNK expression or rather indirect consequences of the altered transcriptional

activity of transcription factors such as Fra-1. Moreover, some of the most significantly altered genes after HA-FRNK expression (Supplemental Table 2) are not included in the affected gene ontologies. In this respect, it is worthwhile to mention that FAK is involved in the generation of the second messengers phosphatidylinositol phosphates (PIP3/PIP2), via recruitment of PI3K to its phosphorylated tyrosine residue (Tyr397) eventually resulting in activation of Akt (8,9). In our hands, Akt1 was significantly downregulated by HA-FRNK expression (Supplemental Table 2). Interestingly, we have previously shown that doxorubicin-induced phosphorylation of Akt1 (PKB) is inhibited by expression of FRNK *in vitro* (7). Therefore, HA-FRNK expression, by disturbing the PI3K pathway, could interfere in an alternative mechanism with tumor cell resistance towards doxorubicin. Further systematic research will be essential to test all individual downstream candidate effectors of FAK signaling that we have here identified.

In conclusion, our data indicate that modulation of FAK *in vivo* can sensitize breast tumor cells towards classical anticancer drugs. Therefore, future targeted pharmacological intervention with FAK inhibitors (33) may become an attractive way to combat otherwise resistant metastatic breast tumors.

ACKNOWLEDGEMENTS

We thank all members in the Division of Toxicology for their helpful discussions and Erik Danen for critically reading the manuscript. This work was supported by grants from the Dutch Cancer Society (KWF 2001-2477) and the EU MetaFight project (HEALTH-F2-2007-201862).

REFERENCES

1. Oktay MH, Oktay K, Hamele-Bena D et al. (2003) Hum Pathol 34:240
2. Owens LV, Xu L, Craven RJ et al. (1995) Cancer Res 55:2752
3. Lahlou H, Sanguin-Gendreau V, Zuo D et al. (2007) PNAS 104:20302
4. McLean GW, Brown K, Arbuckle M et al. (2001) Cancer Res 61:8385
5. van Nimwegen MJ, Verkoeijen S, van Buren L et al. (2005) Cancer Res 65:4698
6. Mitra SK, Lim ST, Chi A et al. (2006) Oncogene 25:4429
7. van Nimwegen MJ, Huigsloot M, Camier A et al. (2006) Mol Pharmacol 70:1330
8. McLean GW, Carragher NO, Avizienyte E et al. (2005) Nat Rev Cancer 5:505
9. van Nimwegen MJ and van de Water B (2007) Biochem Pharmacol 73:597
10. van de Water B, Houtepen F, Huigsloot M et al. (2001) J Biol Chem 276: 36183
11. Xia H, Nho RS, Kahm J et al. (2004) J Biol Chem 279:33024
12. Xu LH, Yang X, Craven RJ et al. (1998) Cell Growth Differ 9:999
13. Halder J, Landen CN Jr., Lutgendorf SK et al. (2005) Clin Cancer Res 11: 8829
14. Halder J, Kamat AA, Landen CN Jr. et al. (2006) Clin Cancer Res 12:4916
15. Duxbury MS, Ito H, Benoit E et al. (2003) Biochem Biophys Res Commun 311:786
16. Tsutsumi K, Kasaoka T, Park HM et al. (2008) Int J Oncol 33:215
17. Ozanne BW, Spence HJ, McGarry LC et al. (2006) Oncogene 26:1
18. Chiappetta G, Ferraro A, Botti G et al. (2007) BMC Cancer 7:17
19. Belguise K, Kersual N, Galtier F et al. (2004) Oncogene 24:1434
20. Lombaerts M, van Wezel T, Philippo K et al. (2006) Br J Cancer 94:661
21. Vial E, Sahai E and Marshall CJ. (2003) Cancer Cell 4:67
22. Casalino L, Bakiri L, Talotta F et al. (2007) EMBO J 26:1878
23. Hamdi M, Popeijus HE, Carlotti F et al. (2008) DNA Repair 7:487
24. Huigsloot M, Tijdens IB, Mulder GJ et al. (2001) Biochem Pharmacol 62:1087
25. Huigsloot M, Tijdens, IB, Mulder GJ et al. (2002) J Biol Chem 277:35869
26. Toyota N, Strebel FR, Stephens LC et al. (1998) Int J Cancer 76:499
27. Matsuo K, Owens JM, Tonko M et al. (2000) Nat Genet 24:184
28. de Graauw M, Tijdens I, Cramer R et al. (2005) J Biol Chem 280:29885

29. Huigsloot M, Tijdens IB, and van de Water B. (2003) Mol Pharmacol 64:965
30. Blick T, Widodo E, Hugo H et al. (2008) Clin Exp Metastasis 25:629
31. Vial E and Marshall CJ. (2003) J Cell Sci 116:4957
32. Mitra SK, Mikolon D, Molina J et al. (2006) Oncogene 25:5969
33. Roberts WG, Ung E, Whalen P et al. (2008) Cancer Res 68:1935
34. Birbach A, Bailey ST, Ghosh S et al. (2004) J Cell Sci 117:3615

SUPPLEMENTAL DATA

Supplemental table 1. Experimental set-up for MTLn3-tetFRNK microarrays.

Annotation	Cell line	doxycycline	# of arrays
Tet-on	MTLn3-tet-on	-	3
Tet-on-doxy	MTLn3-tet-on	+	3
Control	MTLn3-tetFRNK	-	3
FRNK	MTLn3-tetFRNK	+	3

Supplemental table 2. FRNK-induced alterations in annotated genes in MTLn3-tetFRNK cells. Selection of annotated genes is based on the following criteria: $p<0.05$ and Fold Change (FC) >1.5 or <0.67. Left column: downregulated genes, right column: upregulated genes. Lists are sorted by p-values.

Probe_ID	Gene_Symbol	p-value	FC	Probe_ID	Gene_Symbol	p-value	FC
21856159	Cd3d	0.0010	0.320	22403212	Slc1a7	0.0003	2.703
21936000	Ehhadh	0.0013	0.205	22324795	Ch25h_predicted	0.0008	3.521
22393188	Maf	0.0020	0.536	20943419	Cck	0.0011	3.003
20780557	Havcr1	0.0030	0.452	21321652	DOXL1	0.0015	1.946
21031326	Slc17a1	0.0032	0.453	22327267	Bcl2l12_predicted	0.0015	2.591
21201447	Erbb3	0.0045	0.490	21726405	Csf3r_predicted	0.0017	2.358
20762938	Egfl9_predicted	0.0052	0.548	21267977	Igsf4b_predicted	0.0023	3.663
21336348	Dhrs9	0.0053	0.493	21927201	Olr1468	0.0027	3.226
21784618	Il16	0.0054	0.377	20763458	Crebl2_predicted	0.0030	2.114
21849152	F2r	0.0059	0.597	20752903	Cd7_predicted	0.0034	2.079
21748787	Tnks_predicted	0.0060	0.450	21979282	Ndr4	0.0034	2.000
21743859	Eif2c2	0.0064	0.605	21770029	Slc34a3	0.0038	2.532
21788095	Prkaca	0.0065	0.564	21476914	Cldn23_predicted	0.0042	1.931
21282318	Olr859_predicted	0.0078	0.342	20879943	Pgam2	0.0047	1.890
20788184	Pigm	0.0079	0.566	22014663	Sirt1_predicted	0.0053	1.761
21940318	Wisp1	0.0094	0.611	20777806	Tcf15_predicted	0.0055	2.155
21231240	Gmps_predicted	0.0094	0.591	21631081	Cyp2a2	0.0064	3.571
21565791	LOC361237	0.0098	0.573	21215224	Pias3	0.0081	2.849
21876989	Vat1_predicted	0.0101	0.601	20930584	Ubtf	0.0084	2.375
22227921	Kptn_predicted	0.0103	0.507	22391474	Selenbp1	0.0086	1.953
21105219	Cdc25b	0.0105	0.500	20991663	Pfas_predicted	0.0092	1.642
21998913	Dapk2_predicted	0.0105	0.586	21276979	Sftpd	0.0138	1.761
20779692	Zfp238	0.0106	0.450	22395853	Sox18_predicted	0.0144	1.859
22381611	Dlc2	0.0116	0.585	21569506	Palmd_predicted	0.0155	1.880
21574843	Slk	0.0127	0.614	21848369	Cacna1a	0.0157	2.381
21944508	Axl_predicted	0.0133	0.569	21507225	Ka40	0.0160	2.020

Probe_ID	Gene_Symbol	p-value	FC	Probe_ID	Gene_Symbol	p-value	FC
21503808	Fbxl12_predicted	0.0133	0.614	20990619	Olr567_predicted	0.0161	1.845
21200143	Slc35d1_predicted	0.0141	0.619	21960505	Ghr	0.0161	1.742
20880470	Mapre3	0.0142	0.561	21761328	C1qb	0.0167	1.672
21600070	Mrps10_predicted	0.0146	0.660	20700469	Pnrc1	0.0169	1.721
21270267	Akap1	0.0151	0.649	21136726	Guca2a	0.0172	1.661
20910301	Slc25a14	0.0152	0.597	20846089	Thea_predicted	0.0177	1.639
22262479	Tle4	0.0153	0.556	21997485	Rtn3	0.0180	2.899
21944206	Pik3c2b_predicted	0.0154	0.613	20905752	Cplx1	0.0183	2.183
21075257	Cask	0.0159	0.518	21847074	MGC72957	0.0190	1.953
22120455	Akt1	0.0159	0.472	22126943	Aqp6	0.0209	1.558
21545404	Ppt2	0.0167	0.587	21142883	Dhrs3_predicted	0.0212	1.667
21310129	Okl38	0.0168	0.633	21255269	Pygm	0.0221	2.183
22135944	Gna12	0.0174	0.556	22287230	Lin10	0.0224	2.273
21742615	Rrm1	0.0178	0.154	20997792	Tagln3	0.0231	1.799
21548145	Slc16a2	0.0180	0.447	21902211	Hbp1	0.0237	1.661
22289377	Ptpn12	0.0185	0.555	20794054	Mfap3	0.0254	2.336
21661580	Hk2	0.0188	0.623	21137211	Wfdc1	0.0255	1.558
20828341	Acsl1	0.0188	0.621	21325545	Mmp15_predicted	0.0266	1.739
21978152	Cln5_predicted	0.0189	0.652	22267496	RGD1306702_predicted	0.0267	1.773
21833350	LOC286990	0.0190	0.533	20859138	Aldh3a1	0.0276	1.613
21400107	Rab40c	0.0193	0.550	21379704	Knsl8_predicted	0.0282	1.603
21851217	Card10_predicted	0.0193	0.608	21003922	Cabc1_predicted	0.0289	1.560
21959286	Taf1a_predicted	0.0208	0.615	22117376	Usp30_predicted	0.0292	1.639
21159331	Oit3	0.0209	0.639	22373953	LOC60665	0.0299	1.792
22407543	Ggcx	0.0213	0.521	21315820	RGD1308955_predicted	0.0304	1.736
21155260	Nucb2	0.0216	0.445	22351471	RGD1309459_predicted	0.0321	1.721
21010472	Usp38_predicted	0.0221	0.657	20743259	Cda08	0.0325	2.083
20821908	Myh9	0.0222	0.637	22120457	RGD1311107_predicted	0.0326	1.912
21372799	Il17f_predicted	0.0225	0.529	22372665	Exo1_predicted	0.0327	1.786
22243043	RGD1310520_predicted	0.0231	0.602	21035433	Ccl20	0.0329	1.795
21281328	Cav2	0.0234	0.648	20904552	Cldn15_predicted	0.0345	2.463
20824132	Ankrd1	0.0241	0.625	20888760	Olr1337_predicted	0.0347	1.718
21603659	Slc17a6	0.0242	0.562	21220396	Ttc16_predicted	0.0347	1.618
21535209	Cyp3a13	0.0243	0.644	21570101	Cbll1_predicted	0.0349	1.592
21622250	Thap6_predicted	0.0244	0.483	20737316	Gpr124_predicted	0.0355	2.268
21876288	Lrp8_predicted	0.0249	0.624	21306709	RGD1306952_predicted	0.0361	1.957
22139518	Etsrp71_predicted	0.0249	0.581	21954151	Ccng2_predicted	0.0374	1.686
22336310	***Junb***	0.0251	0.639	22097357	MGC94550	0.0375	1.520
22136467	Phf15_predicted	0.0273	0.458	22358977	Hapln4_predicted	0.0410	1.876
21314484	Lgals9	0.0276	0.630	21849031	Cox6c	0.0422	1.730
21160091	Slc4a11_predicted	0.0279	0.631	20876655	Nr1h4	0.0441	1.901

Probe_ID	Gene_Symbol	p-value	FC	Probe_ID	Gene_Symbol	p-value	FC
22282806	Lrrc15	0.0282	0.323	21417467	Cacna1b	0.0446	1.538
21305806	***Fosl1***	0.0284	0.564	22175193	Wt1	0.0447	1.901
21219586	Pou2f2	0.0287	0.656	21176640	Tpbg	0.0465	1.536
21897732	Stambp	0.0291	0.658	20854804	Ka17	0.0470	1.499
20876299	Rnf40	0.0293	0.644	20868496	Sod2	0.0475	1.667
21006903	Exoc8	0.0301	0.639	20737825	Notch4	0.0476	1.577
21588690	Nefh	0.0307	0.576	20752295	Tep1	0.0479	1.555
21968384	Fcnb	0.0308	0.540	21584298	Dpp8_predicted	0.0482	1.504
22207768	Mdh1b_predicted	0.0313	0.400	21549591	Siah1a	0.0495	1.580
21110267	Madh3	0.0313	0.456				
21890138	Znf629_predicted	0.0323	0.559				
22288872	Gk-rs1_predicted	0.0324	0.571				
21404310	Hnrpr	0.0332	0.656				
21875776	Nmt2	0.0337	0.665				
21137506	Fkbp14_predicted	0.0341	0.612				
21233599	Tcfe2a	0.0347	0.473				
20875200	Np	0.0353	0.574				
20826517	Meox1_predicted	0.0361	0.353				
20780470	Pim1	0.0367	0.641				
21952268	Klre1	0.0371	0.574				
20989100	Ppargc1a	0.0373	0.590				
21929390	Lgals5	0.0381	0.629				
21113865	Il24	0.0382	0.556				
21985561	Lcn7	0.0385	0.655				
20862355	Rufy1_predicted	0.0388	0.574				
21396873	Ctrl	0.0389	0.650				
21620770	Nppb	0.0389	0.495				
22067183	Epn2	0.0392	0.656				
21591414	RGD1305424_predicted	0.0402	0.404				
21132402	Phospho1_predicted	0.0405	0.667				
21154733	Npl4	0.0406	0.635				
22035995	Fgd3_predicted	0.0407	0.642				
21481266	Dnaja2	0.0415	0.626				
22066307	Actn4	0.0422	0.661				
21239072	Fbxl14_predicted	0.0423	0.667				
21288312	Upb1	0.0431	0.575				
21549672	Hrasls3	0.0431	0.568				
21289633	Dbt	0.0432	0.477				
21466445	Synj2	0.0434	0.644				
21271425	Tufm_predicted	0.0441	0.647				
21995038	Phlda1	0.0443	0.662				

Probe_ID	Gene_Symbol	p-value	FC
21497995	Procr_predicted	0.0446	0.666
21388641	Hmmr	0.0453	0.667
20884920	LOC493574	0.0458	0.623
21378546	Tnpo2_predicted	0.0459	0.604
21535218	Car7_predicted	0.0467	0.518
21418355	Mgat5	0.0473	0.611
22413236	Pdrp	0.0478	0.656
21033847	Rap2b	0.0479	0.617
21513568	Loxl2_predicted	0.0480	0.640
21921832	Clc	0.0482	0.648
22104079	Abhd2_predicted	0.0482	0.631
21700036	Tagln	0.0485	0.407
21204716	Slc4a2	0.0491	0.648
21918636	Pdlim7	0.0493	0.510
21667412	Mef2d	0.0493	0.614
21153498	MGC94736	0.0497	0.639

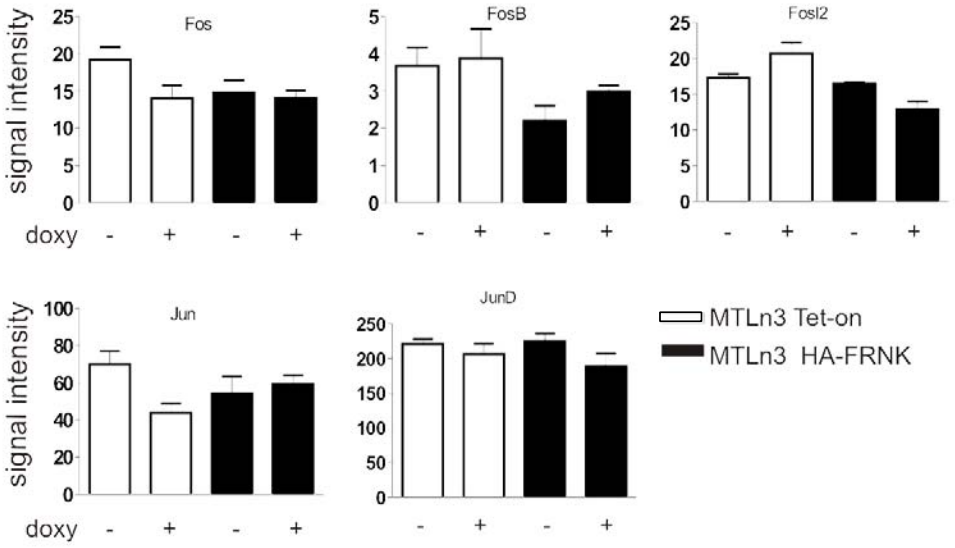

Supplemental figure 1. HA-FRNK-dependent gene expression of Fos and Jun family members. Expression values of Fos an Jun family members (other than FosL and JunB) in MTLn3-tet-on and MTLn3-tetFRNK cells treated with doxycycline or left untreated, as determined in the microarray studies.

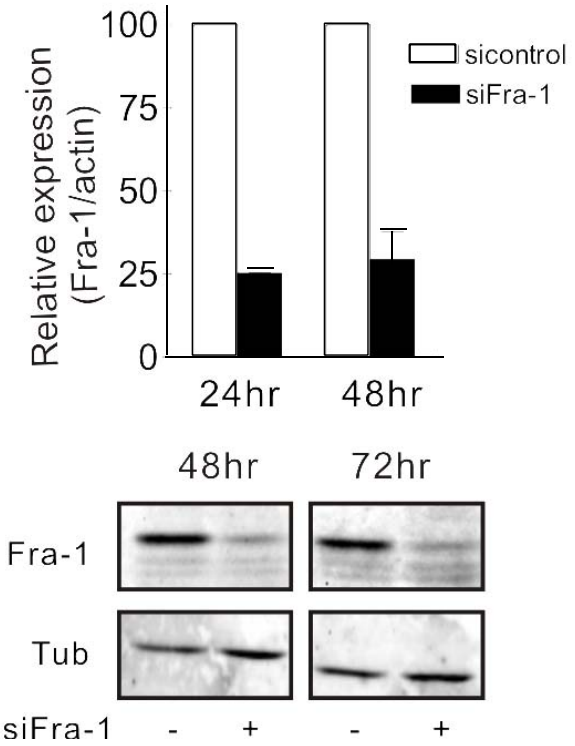

Supplemental figure 2. Analysis of siRNA-mediated Fra-1 knockdown. MTLn3 cells were transfected with siFra-1 and 24 or 48 hours later, *fra-1* mRNA was determined by qRT-PCR using actin as an internal control (upper panel). Fra-1 protein expression was determined by Western blot analysis (lower panel).